24
Boundary layers

WARNING: unfinished

Between the two extremes of sluggish creeping flow at low Reynolds number and lively ideal flow at high, there is a regime in which neither is dominant. At large Reynolds number, the flow will be nearly ideal over most of space, except near solid boundaries where the no-slip condition requires the speed of the fluid to match the speed of the boundary wall. Here will arise transition layers in which the flow velocity changes rapidly from the velocity of the wall to the velocity of the flow in the fluid at large. Boundary layers are typically thin compared to the radius of curvature of the solid walls, and that simplifies the basic equations.

In a boundary layer the character of the flow thus changes from creeping near the boundary to ideal far from it. The most interesting and also most difficult physics characteristically takes place in such transition regions. But humans live out their lives in nearly ideal flows of air and water at Reynolds numbers in the millions with boundary layers only millimeters thick, and are normally not conscious of them. Smaller animals eking out a turbulent existence at the surface of a stone in a river may be much more aware of the vagaries of boundary layer physics which may influence their body shapes and internal layout of organs.

Ludwig Prandtl (1875–1953). *German physicist, often called the father of aerodynamics. Contributed to wing theory, streamlining, compressible subsonic airflow, and turbulence.*

Boundary layers serve to insulate bodies from the ideal flow that surrounds them. They have a "life of their own" and may separate from the solid walls and wander into regions containing only fluid. Detached layers may again split up, creating complicated unsteady patterns of whirls and eddies. Advanced understanding of fluid mechanics begins with the understanding of boundary layers. Systematic boundary layer theory was first advanced by Prandtl in 1904 and has in the 20'th century become a major subtopic of fluid mechanics [50, 51].

In this chapter we shall mainly focus on the theory of incompressible laminar boundary layers without heat flow, together with a semi-empirical discussion of turbulence.

Copyright © 1998–2002, Benny Lautrup

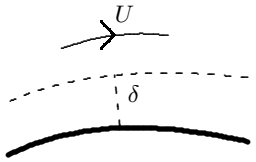

The transition from zero velocity at the wall to the mainstream velocity U mostly takes place in a layer of finite thickness δ.

24.1 Physics of boundary layers

Consider a nearly ideal flow with velocity U along a solid wall at rest. The Reynolds number is as usual calculated as $\mathsf{Re} \approx UL/\nu$ where L is a typical length scale for significant changes in the flow, determined by the geometry of bodies and containers. The no-slip condition requires the velocity to vary from zero right at the wall to U in the flow at large. Under many — but not all— circumstances, this transition will for $\mathsf{Re} \gg 1$ take place in a thin *boundary layer* of thickness $\delta \ll L$.

Close to the wall, the velocity field is tiny because of the no-slip condition. The flow pattern will in this region always be laminar, in fact creeping, with the parallel (streamwise) velocity rising linearly from zero. The laminar flow may extend all the way to the edge of the boundary layer, or the flow may at sufficiently high Reynolds number become turbulent.

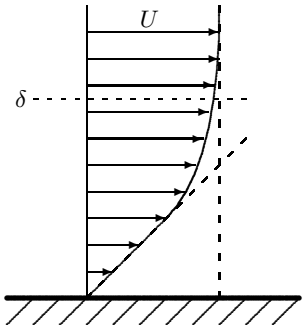

Sketch of the flow in a laminar boundary layer with constant mainstream flow. The velocity rises linearly close to the solid wall but veers off to match the mainstream flow velocity U at a characteristic distance δ from the wall. The precise layer thickness depends on a choice of what one means by "matching" the mainstream flow.

Laminar boundary layer thickness

The effective Reynolds number in a steady laminar boundary layer can be estimated from the ratio of advective to viscous terms in the Navier-Stokes equation,

$$\frac{|(\boldsymbol{v}\cdot\boldsymbol{\nabla})\boldsymbol{v}|}{\left|\nu\boldsymbol{\nabla}^2\boldsymbol{v}\right|} \sim \frac{U^2/L}{\nu U/\delta^2} = \frac{U\delta^2}{\nu L} = \frac{\delta^2}{L^2}\mathsf{Re}\,. \tag{24-1}$$

Here the numerator was estimated from the change in mainstream velocity along the wall over a distance L, using that the flow in a laminar layer must follow the geometry of the mainstream flow. The denominator was estimated from the rapid change in velocity across the thickness δ of the boundary layer.

The boundary layer is characterized by the transition from viscous dominance near the wall to advective dominance in the mainstream. We estimate the *boundary layer thickness* by requiring the effective Reynolds number (24-1) to be around unity, leading to

$$\boxed{\delta \sim \sqrt{\frac{\nu L}{U}} = \frac{L}{\sqrt{\mathsf{Re}}}}\,. \tag{24-2}$$

This estimate is valid up to a coefficient of order unity which will be discussed later (section 24.4). For large mainstream Reynolds number, $\mathsf{Re} \gg 1$, the thickness of the boundary layer will thus be considerably smaller than the typical length scale of the mainstream flow.

> The Reynolds numbers for flows we encounter in daily life easily reach into the millions, making the boundary layer thickness smaller than a thousandth of the scale of the flow. Jogging or swimming, one hardly notices the existence of boundary layers that are only millimeters thick. The pleasant tingling skin sensation you experience from streaming air or water comes presumably from the complex flow at larger scale generated by the irregular shape of your body.

Copyright © 1998–2002, Benny Lautrup

Wall shear stress

In the laminar boundary layer, the velocity rises linearly with the distance from the boundary. The normal velocity gradient at the wall is approximately $\lambda \approx U/\delta$, and multiplying with the viscosity we obtain an estimate of the shear stress on the wall,

$$\sigma_{\mathsf{wall}} = \eta\lambda \approx \eta\frac{U}{\delta} \sim \frac{\rho_0 U^2}{\sqrt{\mathsf{Re}}} \; . \tag{24-3}$$

In the last expression we have also used the steady-flow estimate (24-2). The wall stress determines the *skin drag*, $\mathcal{D} = \int_A \sigma_{\mathsf{wall}}\, dS$, on a flat surface of area A. The wall stress decreases with increasing Reynolds number, in agreement with the diminishing influence of viscosity at higher Reynolds numbers.

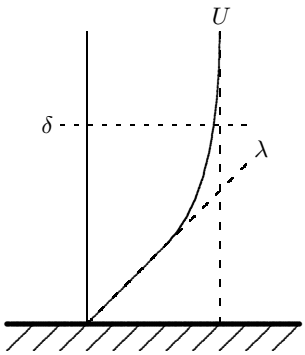

The stress on the wall of a laminar boundary layer is determined by the slope $\lambda \approx U/\delta$ of the linearly rising velocity near the wall.

Initial viscous growth

When a body in steady flow suddenly changes its velocity, the fluid immediately surrounding it will have to follow along in order to satisfy the no-slip boundary condition. Large velocity gradients and therefore large stresses will develop in the fluid next to the body, and these stresses will cause fluid layers farther out also to be dragged along. Eventually this process may come to and end and the flow will once again be steady. In the beginning the newly created boundary layer is extremely thin, so that the general geometry of the flow and the shape of the body must be unimportant. This indicates that suddenly created boundary layers always start out their growth in the same universal way.

Suppose that both body and fluid initially are at rest, and that the body at $t = 0$ is suddenly set into motion with velocity U. If the boundary layer at time $t > 0$ has reached a thickness $\delta(t)$, the fluid in the boundary layer will on the average have changed its velocity from 0 to about $\frac{1}{2}U$ in time t. This makes the local acceleration of order U/t (disregarding factors 1/2) and allows us to estimate the ratio between the local and inertial acceleration

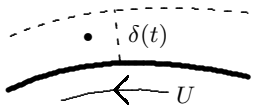

The wall is suddenly set into motion. After a time t, the velocity at a point in the middle of the growing boundary layer has changed from 0 to $\frac{1}{2}U$.

$$\frac{|\partial \boldsymbol{v}/\partial t|}{|(\boldsymbol{v}\cdot\boldsymbol{\nabla})\boldsymbol{v}|} \approx \frac{U/t}{U^2/L} = \frac{L}{Ut} \; . \tag{24-4}$$

The time the fluid takes to pass the body is L/U. For times much shorter than this, $t \ll L/U$, the inertial acceleration term can be disregarded relative to the local acceleration, and the boundary layer will continue to grow. The boundary layer cannot "go steady" until it is much older than the passing time.

In a "young" boundary layer with $t \ll L/U$, the advective acceleration can thus be disregarded, and the physics is controlled by the ratio of local to viscous acceleration,

$$\frac{|\partial \boldsymbol{v}/\partial t|}{|\nu\boldsymbol{\nabla}^2\boldsymbol{v}|} \approx \frac{U/t}{\nu U/\delta^2} = \frac{\delta^2}{\nu t} \; . \tag{24-5}$$

Copyright © 1998–2002, Benny Lautrup

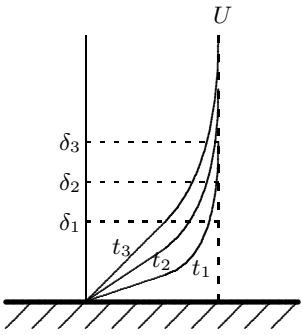

Initial growth of a laminar boundary layer. The three velocity profiles correspond to increasing times $t_1 < t_2 < t_3$ and increasing thicknesses $\delta_1 < \delta_2 < \delta_3$.

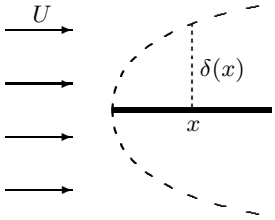

A semi-infinite plate in an otherwise uniform flow. The dashed curve is the estimated parabolic boundary layer shape.

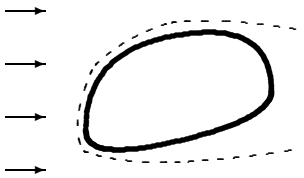

Sketch of the boundary layer around a bluff body in steady uniform flow. On the windward side the boundary layer is thin, whereas it widens and tends to separate on the lee side. In the channel formed by the separated boundary layer, unsteady flow patterns may arise.

This should be of order unity in the boundary layer, leading to

$$\boxed{\delta \sim \sqrt{\nu t} \qquad \text{for } t \ll L/U} \,. \tag{24-6}$$

A suddenly created boundary layer always starts out like this, growing with the squareroot of time. This behavior is as we have seen before typical of viscous diffusion processes, and in is of same form as the estimate of the rate of momentum diffusion (page 289) and the core expansion rate of a decaying vortex (page 361).

After the initial universal growth, the boundary layer comes to depend on the general geometry of the flow for $t \approx L/U$, when it reaches the thickness (24-2). It takes more careful analysis to see whether the flow eventually settles down into a steady boundary layer, or whether instabilities arise, leading to a radical change in the character of the flow such as boundary layer separation or turbulence.

Influence of body geometry

The simplest geometry in which a steady boundary layer can be studied is a semi-infinite plate with its edge orthogonal to a uniform mainstream flow (we shall solve this case analytically in section 24.4). Here the only possible length scale is the distance x from the leading edge, so that we must have

$$\delta \sim \sqrt{\frac{\nu x}{U}} \,. \tag{24-7}$$

This shows that boundary layers tend to grow thicker downstream, even if the mainstream flow is completely uniform and independent of x. If the flat plate is set abruptly into motion, the initial growth of the layer at a downstream distance x steadies at time $t \approx x/U$. Disregarding sound waves, the time $t = x/U$ is also the earliest moment that the edge causally can influence the flow near x. Intuitively one might say that the viscous growth of the boundary layer is curtailed by the encounter with the blast of undisturbed fluid coming in from afar.

Boundary layers have a natural tendency towards *downstream thickening*, because they build up along a body in a cumulative fashion. Having reached a certain thickness, a boundary layer acts as a not-quite-solid "wall" on which another boundary layer will form. The thickness of a steady boundary layer is also strongly dependent on whether the mainstream flow is accelerating or decelerating along the body, behavior which in turn is determined by the geometry. If the mainstream flow accelerates, *i.e.* grows with x, the boundary layer tends to remain thin. This happens at the front of a moving body, where the fluid must speed up to get out of the way. Conversely, towards the rear of the body, where the mainstream flow again decelerates in order to "fill up the hole" left by the passing body, the boundary layer becomes rapidly thicker, and may even separate from the body, creating an unsteady, often turbulent, *trailing wake*.

Copyright © 1998–2002, Benny Lautrup

Merging boundary layers

The increase of a boundary layer's thickness with body size implies for an infinite body that the boundary layer must be infinitely thick or at least so thick that it fills out all the available space. In steady planar flow between moving plates (section 17.1), the velocity profile of the fluid interpolates linearly between the plate velocities, and one sees nothing like a boundary layer with finite thickness near the plates. In pressure-driven steady pipe flow (section 18.6), the exact shape of the Poiseuille velocity profile is parabolic (as long as the flow is laminar), whatever the viscosity of the fluid. Again we see no trace of a finite boundary layer in the exact solution.

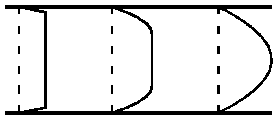

Sketch of the shape of the velocity profile in pressure-driven flow between half-infinite plates at various distances downstream from the entrance at the left.

Consider now pressure-driven flow between two half-infinite plates, a distance d apart. The boundary layers grow like $\sqrt{x}$ from both sides downstream from the entrance and eventually merge with each other at a typical distance $x = L'$, called the *entrance length*. Further downstream, the Poiseuille profile is established, and the distinction between boundary and mainstream flow is no more possible. The two boundary layers meet at $x = L'$, determined by solving the equation $2\delta(x) \approx d$. Using a conservative estimate $\delta(x) \approx 3\sqrt{\nu x/U}$, the entrance length becomes

$$L' \approx \frac{d}{36}\,\mathsf{Re} \tag{24-8}$$

with $\mathsf{Re} = Ud/\nu \gg 1$. The numerical computation in section 19.4 showed that this estimate is in fact not far off the mark.

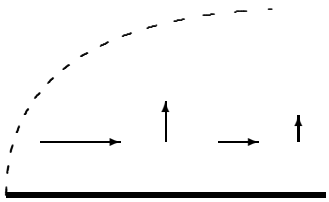

The thickening of a boundary layer decelerates the flow and leads to upwelling of fluid from the boundary.

Upwelling and downwash

Inside a boundary layer, at a fixed distance from a flat solid wall with a uniform mainstream velocity U, the flow decelerates downstream as the boundary layer thickens due to the action of viscosity. Mass conservation requires a compensating *upwelling* of fluid into the fluid at large. If the boundary is permeable and fluid is sucked down through it at a constant rate, the upflow can be avoided, and a steady boundary layer of constant thickness may be created (problem 24.1).

The mainstream flow is determined by bodies and containers that guide the fluid and will generally not be uniform but rather accelerate or decelerate along the boundaries. An accelerating mainstream flow will counteract the natural deceleration in the boundary layer and may even overwhelm it, leading to a *downwash* towards the boundary. Mainstream acceleration thus tends to stabilize a boundary layer so that it has less tendency to thicken, and may lead to constant or even diminishing thickness. Conversely, if the mainstream flow decelerates, this will add to the natural deceleration in the boundary layer and increase its thickness as well as the upwelling.

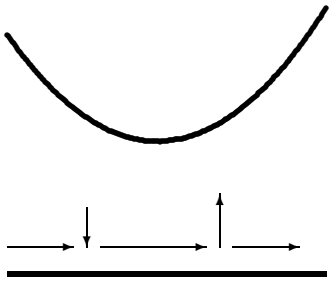

Mainstream acceleration in a converging channel produces a downwash of fluid, and conversely in a diverging channel.

Copyright © 1998–2002, Benny Lautrup

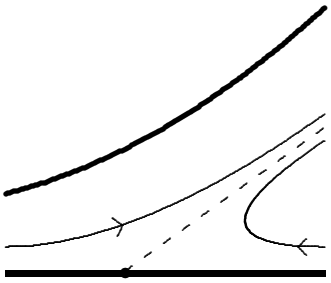

Flow reversal and boundary layer separation in a diverging channel with decelerating flow.

Separation

Even at very moderate mainstream deceleration, the upwelling can become so strong at some point that the fluid flowing in the mainstream direction cannot feed it. Some of the fluid in the boundary layer will then have to flow against the mainstream flow. Between the forward and reversed flows there will be a separation line ending on the wall. Such *flow reversal* was also noticed in lubrication (page 393), although there are no boundary layers in creeping flow.

In the region of reversed flow, the velocity still has to vanish right at the boundary. Moving up from the boundary wall, the flow first moves backwards with respect to the mainstream, but farther from the wall it must again turn back to join up with the mainstream. The velocity gradient must accordingly be negative right at the boundary in the reversal region, corresponding to a negative wall stress σ_{wall}. The vanishing of the wall stress, $\sigma_{\mathsf{wall}} = 0$, indicates that boundary layer separation may happen. It is not a sufficient condition, because flow reversal can in principle be a local phenomenon taking place entirely within the boundary layer, as may be the case if there is a dent in the wall.

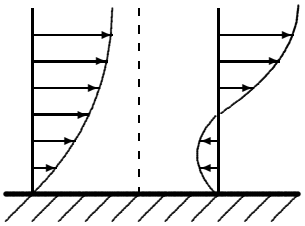

Velocity profiles before and after the separation point (dashed line).

Turbulence

Boundary layers can also become turbulent. Turbulence efficiently mixes fluid in all directions. The orderly layers of fluid that otherwise isolate the wall from the mainstream flow all but disappear, and on average, the mainstream velocity will press much closer to the wall. Turbulence typically sets in downstream from the front of body when the laminar boundary layer has grown so thick that the *local Reynolds number*

$$\mathsf{Re}_\delta = \frac{U\delta}{\nu} \ , \tag{24-9}$$

becomes large enough, say in the thousands.. In a laminar boundary layer, the estimate (24-2) shows that $\mathsf{Re} \sim \mathsf{Re}_\delta^2$, so that turbulence will not arise until the mainstream Reynolds number reaches into the millions, which incidentally is just about the range in which humans and many of their machines operate.

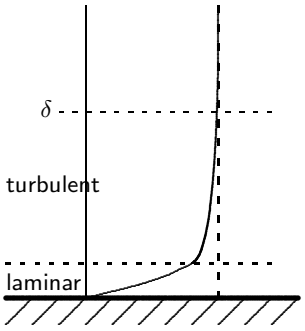

In a turbulent boundary layer there will always be a thin nearly laminar sublayer, in which the velocity profile rises linearly from the wall.

Although the turbulent velocity fluctuations press close to the wall, there will always remain a thin viscous, nearly laminar, sublayer close to the wall, in which the average velocity gradient normal to the wall rises linearly with distance. Since the mainstream velocity on average comes much closer to the wall, the average wall stress will be much larger than in a completely laminar boundary layer. The skin drag on a body is consequently expected to increase when the boundary layer becomes turbulent, though other changes in the flow may interfere and instead cause an even larger drop in the form drag at a particular value of the Reynolds number, as we saw in the discussion of the "drag crisis" (page 381).

The phenomenology of turbulent boundary layers is discussed in some detail for a flat plate in section 24.5.

Copyright © 1998–2002, Benny Lautrup

24.2 Growth of a boundary layer

The initial growth of the boundary layer near a flat plate which is suddenly set into motion (Stokes first problem) must also follow the universal law (24-6). In this case there is no intrinsic length scale for the geometry, and the transition to geometry-dependent steady flow cannot take place. The planar boundary layer (called the Stokes layer) can for this reason be expected to provide a clean model for universal viscous growth.

Analytic solution

As usual it is more convenient to view the plate from the reference frame in which the plate and the fluid initially move with the same velocity U and the plate is suddenly stopped at $t = 0$. Assuming that the flow is planar with $v_x = v_x(y,t)$ and $v_y = 0$, the Navier-Stokes equation for incompressible flow reduces to the momentum-diffusion equation (17-7), which is repeated here for convenience

$$\frac{\partial v_x}{\partial t} = \nu \frac{\partial^2 v_x}{\partial y^2} \ . \tag{24-10}$$

The linearity of this equation guarantees that the velocity everywhere must be proportional to U, and since there is no intrinsic length or time scale in the definition of the problem, the velocity field must be of the form,

$$v_x(y,t) = U f(s) \ , \qquad s = \frac{y}{\sqrt{2\nu t}} \tag{24-11}$$

where the so far unknown function $f(s)$ should obey the boundary conditions $f(0) = 0$ and $f(\infty) = 1$. The factor 2 in the squareroot is conventional.

Upon insertion of (24-11) into (24-10) we are lead to an ordinary second order differential equation for $f(s)$,

$$\boxed{f''(s) = -s f'(s)} \ . \tag{24-12}$$

Viewed as a first order equation for $f'(s)$, it has the unique solution $f'(s) \sim \exp(-s^2/2)$. Integrating this expression once more over s and applying the boundary conditions, the final result becomes

$$f(s) = \sqrt{\frac{2}{\pi}} \int_0^s e^{-s'^2/2} \, ds' = \mathrm{erf}\left(\frac{s}{\sqrt{2}}\right) \ , \tag{24-13}$$

where $\mathrm{erf}(\cdot)$ is the well-known error function. For small values of s we have $f(s) \approx s\sqrt{2/\pi}$ whereas for large values the function approaches 1 with a Gaussian tail, $1 - f(s) \sim \exp(-s^2/2) = \exp(-y^2/4\nu t)$, typical of momentum diffusion (see page 289).

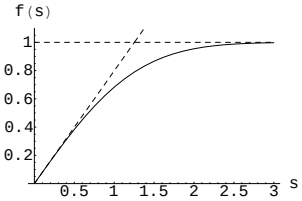

Plot of $f(s)$. The sloping dashed line is tangent at $s = 0$ with inclination $f'(0) = \sqrt{2/\pi}$.

Copyright © 1998–2002, Benny Lautrup

Thickness definitions

The velocity field is self-similar in the sense that, apart from the length scale $\sqrt{\nu t}$, it has the same spatial shape $f(y/\sqrt{\nu t})$ as a function of y, at all times. Conventionally, one defines the boundary layer thickness to be

$$\delta = k\sqrt{\nu t} \tag{24-14}$$

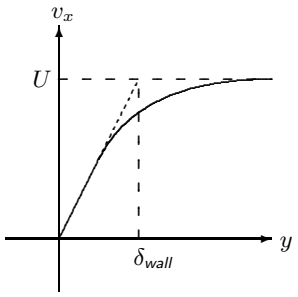

Definition of wall stress thickness from the intercept between the linearly rising velocity at small y and the mainstream velocity U.

where k is a numeric coefficient. Typically a value of k is selected such that a high percentage of the mainstream velocity is obtained at the "edge" $y = \delta$ of the boundary layer. For example, for $k = 3.64277\ldots$ one obtains $f(k) = 99\%$ of the mainstream velocity. To avoid arbitrariness, other definitions of boundary layer thickness have been proposed:

Wall stress thickness: The velocity profile is linear near the wall after which it tapers off towards $f(\infty) = 1$ with a Gaussian tail. The linear part of the velocity profile, $v_x = Uy/\sqrt{\pi\nu t}$, crosses U for $y = \delta_{\mathsf{wall}}$, where

$$\delta_{\mathsf{wall}} = \sqrt{\pi\nu t} \approx 1.7725\sqrt{\nu t}\ , \tag{24-15}$$

At $y = \delta_{\mathsf{wall}}$, we find $v_x/U = f(\sqrt{\pi/2}) \approx 79\%$. From δ_{wall} we obtain the wall shear stress,

$$\sigma_{\mathsf{wall}} = \eta \left.\frac{\partial v_x}{\partial y}\right|_{y=0} = \eta\frac{U}{\delta_{\mathsf{wall}}} = \frac{\eta U}{\sqrt{\pi\nu t}}\ . \tag{24-16}$$

Initially, the wall stress is infinite, but afterwards it decreases with the squareroot of time because of the viscous growth of the boundary layer.

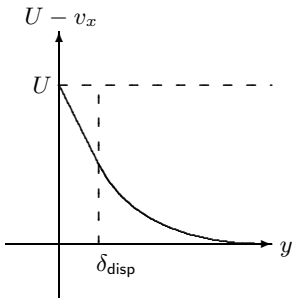

Definition of displacement thickness from the integral of $U - v_x$.

Displacement thickness: Another precise definition of boundary layer thickness is based on the amount of fluid slowed down by the stopped plate. Before the plate is stopped all fluid moves along with velocity U, but eventually it all comes to rest. At any given moment t, the drop in velocity at the distance y from the plate is $U - v_x(y,t)$, and the *loss* in the originally infinite volume discharge rate along the plate becomes (per unit of length in the z-direction)

$$Q(t) = \int_0^\infty (U - v_x(y,t))\, dy\ . \tag{24-17}$$

Initially, the same discharge rate was carried by a layer of thickness

$$\delta_{\mathsf{disp}} = \frac{Q}{U} = \sqrt{2\nu t}\int_0^\infty (1 - f(s))\, ds = \frac{2}{\sqrt{\pi}}\sqrt{\nu t} = 1.128\sqrt{\nu t}\ , \tag{24-18}$$

which is called the *displacement thickness*.

Copyright © 1998–2002, Benny Lautrup

Momentum thickness: Similarly, the instantaneous rate of loss of fluid momentum caused by the stopped plate is (per unit of length in the z-direction)

$$\dot{\mathcal{P}}_x(t) = \int_0^\infty \rho_0(U - v_x(y,t))v_x(y,t)\,dy\ . \tag{24-19}$$

Initially, the same momentum transport rate was carried by a layer of thickness,

$$\delta_{\mathsf{mom}} = \frac{\dot{\mathcal{P}}_x}{\rho_0 U^2} = \sqrt{2\nu t}\int_0^\infty (1-f(s))f(s)\,ds = \frac{2(\sqrt{2}-1)}{\sqrt{\pi}}\sqrt{\nu t} = 0.4674\sqrt{\nu t}\ . \tag{24-20}$$

called the *momentum thickness*.

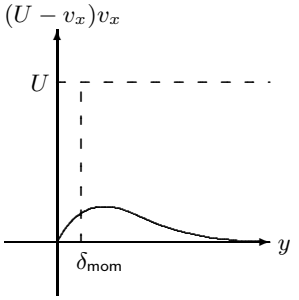

Definition of momentum thickness from the integral of $(U - v_x)v_x$.

The Gaussian tail

Notice that the Gaussian tail of the boundary layer extends all the way to spatial infinity for *any* positive time, $t > 0$. How can that be, when the plate was only brought to stop at time $t = 0$? Won't it take a finite time for this event to propagate to spatial infinity? The short answer is that we have assumed the fluid to be incompressible, and this — fundamentally untenable — assumption will in itself entail infinite signal speeds. At a deeper level, a diffusion equation like (24-10) is the statistical continuum limit of the dynamics of random molecular motion in the fluid, and although extremely high molecular speeds are strongly damped, they may in principle occur. The fundamental upper limit to diffusion speed as well as to incompressibility is, as discussed before, always set by the finite speed of sound.

Vorticity generation

The vorticity field has only one component

$$\omega_z(y,t) = -\frac{\partial v_x(y,t)}{\partial y} = -\frac{U f'(s)}{\sqrt{2\nu t}} = -\frac{U}{\sqrt{\pi\nu t}}e^{-y^2/4\nu t} \tag{24-21}$$

Before the plate stopped, the flow was everywhere irrotational. Afterwards there is evidently vorticity in the boundary layer. Where did it come from?

Consider a (nearly) infinite rectangle with support of length L on the plate. The flow in the boundary layer has a total flux of vorticity (or circulation) $\Gamma = \int \boldsymbol{\omega}\cdot d\boldsymbol{S} = \oint \boldsymbol{v}\cdot d\boldsymbol{\ell}$ through this rectangle. The fluid velocity always vanishes on the plate, is orthogonal to the sides, and approaches the constant U at infinity, so that we obtain $\Gamma = -UL$. Since the circulation is constant in time, vorticity is not generated inside the boundary layer itself during its growth, but rather at the plate surface during the instantaneous deceleration to zero velocity. If the plate did not stop with infinite deceleration, but followed a gentler path $U(t)$ from U to 0, the circulation $\Gamma(t) = (U(t)-U)L$ would also have decreased gently from 0 to $-UL$. The conclusion is that vorticity is originally generated at the plate surface during acceleration and deceleration. Afterwards it diffuses away from the plate and into the fluid at large without changing the total circulation.

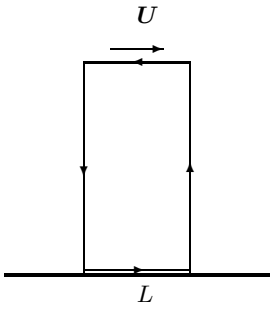

The circulation around an infinitely tall rectangle with side L against the moving wall is $\oint \boldsymbol{v}\cdot d\boldsymbol{\ell} = -UL$.

Copyright © 1998–2002, Benny Lautrup

24.3 Boundary layer theory

In his short 1904 paper [14] Prandtl introduced the concept of boundary layers and pointed out that there were simplifying features, allowing for less complicated equations than the full set of Navier and Stokes. The greater simplicity comes from the assumption of nearly ideal mainstream flow with $\mathsf{Re} \gg 1$, which according to the estimate (24-2) implies that boundary layers are thin, *i.e.* $\delta \ll L$ where L is the length scale for variations in the mainstream flow.

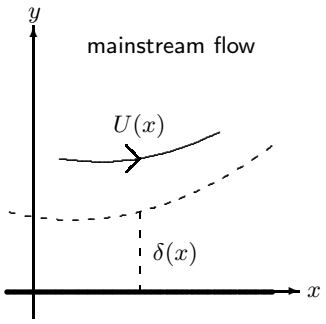

Geometry of two-dimensional planar boundary flow. In the absence of viscosity there would be a slowly varying ideal slip-flow $U(x)$ along the boundary. Viscosity interposes a thin boundary layer of thickness $\delta(x)$ between the slip-flow and the boundary.

We shall — as Prandtl did — consider only the two-dimensional case with an infinitely extended planar boundary wall at $y = 0$ and a unidirectional mainstream flow along x. The analysis can be extended to a curved boundary, as long as the boundary layer is much thinner than the radius of curvature R of the wall, $\delta \ll R$. In that case, the coordinates should be understood as curvilinear with the x-coordinate following the shape of the wall and the y-coordinate always pointing along the local normal.

Ideal slip-flow

In the absence of viscosity, the incompressible ideal fluid would slip along the boundary, $y = 0$, with a slowly varying *slip-velocity*, $v_x = U(x)$. Leaving out gravity, it follows from Bernoulli's theorem (15-12) that there must be an associated slip-flow pressure at the boundary,

$$P(x) = P_0 - \frac{1}{2}\rho_0 U(x)^2 \ , \tag{24-22}$$

where P_0 is a constant. The slip-flow pressure simply reflects the variation in slip-velocity along the boundary. Strictly speaking, there will also be a normal slip-flow component $v_y = V(x)$, created by the upwelling and downwash accompanying the flow in the boundary layer. As will be shown below, this component is usually negligible compared to U.

The no-slip condition demands that the true fluid velocity changes rapidly from $\boldsymbol{v} = \boldsymbol{0}$ right at the boundary, $y = 0$, to $\boldsymbol{v} = (U(x), 0, 0)$ somewhat outside the boundary layer, $y \gtrsim \delta$. The slip-flow velocity $U(x)$ and boundary pressure $P(x)$ describe the fluid in the region $\delta \ll y \ll L$, well outside the boundary layer but still so close to the boundary that the mainstream flow only depends on x. In the mainstream proper for $y \gtrsim L$, flow and pressure depend both on x and y with a typical length scale L for major variations.

Equation of continuity

Integrating the equation of continuity,

$$\frac{\partial v_x}{\partial x} + \frac{\partial v_y}{\partial y} = 0 \ , \tag{24-23}$$

Copyright © 1998–2002, Benny Lautrup

over y, and using the boundary condition $v_y = 0$ for $y = 0$, we obtain,

$$\boxed{v_y(x,y) = -\frac{\partial}{\partial x}\int_0^y v_x(x,y')\,dy'}\,, \tag{24-24}$$

which is an exact relation. It shows that there will in general arise a contribution to the mainstream flow normal to the boundary, even for $y \to \infty$. Since $v_y \approx U\,\delta/L \sim U/\sqrt{\mathsf{Re}}$, this contribution to mainstream upwelling or downwash caused by the boundary layer is normally considerably smaller than the slip-flow.

Prandtl's momentum equation

In two dimensions the x-component of the steady-flow Navier-Stokes equations (18-2) takes the form

$$v_x\frac{\partial v_x}{\partial x} + v_y\frac{\partial v_x}{\partial y} = -\frac{1}{\rho_0}\frac{\partial p}{\partial x} + \nu\left(\frac{\partial^2 v_x}{\partial x^2} + \frac{\partial^2 v_x}{\partial y^2}\right)\,, \tag{24-25a}$$

$$v_x\frac{\partial v_y}{\partial x} + v_y\frac{\partial v_y}{\partial y} = -\frac{1}{\rho_0}\frac{\partial p}{\partial y} + \nu\left(\frac{\partial^2 v_y}{\partial x^2} + \frac{\partial^2 v_y}{\partial y^2}\right)\,. \tag{24-25b}$$

In either of these equations, the double derivative after y is proportional to $1/\delta^2$, whereas the double derivative after x is proportional to $1/L^2$, making it a factor $1/\mathsf{Re}$ smaller, thus allowing us to drop it. From the estimate of the thickness of the boundary layer (24-2) it follows that the viscous terms on the right are of the same order of magnitude as the advective terms on the left. Setting $v_x \approx U$ and $v_y \approx U\delta/L$ we estimate from any of the remaining terms in the second equation that the normal pressure gradient is $\partial p/\partial y \approx \rho_0 U^2\delta/L^2$. Finally, multiplying this expression with δ we obtain the pressure variation across the boundary layer $\Delta_y p \approx \rho_0 U^2\delta^2/L^2 \sim \rho_0 U^2/\mathsf{Re}$. This is much smaller, by a factor $1/\mathsf{Re}$, than the variations in the slip-flow pressure (24-22) and may thus be disregarded.

The true pressure in the boundary layer is essentially equal to the slip-flow pressure, $p(x,y) \approx P(x)$, and we obtain from (24-25a) and (24-22),

$$\boxed{v_x\frac{\partial v_x}{\partial x} + v_y\frac{\partial v_x}{\partial y} = UU' + \nu\frac{\partial^2 v_x}{\partial y^2}}\,, \tag{24-26}$$

where $U' = dU/dx$. This is *Prandtl's momentum equation.* Since v_y is given in terms of v_x by the continuity equation (24-24), we have obtained a single integro-differential equation which for any given $U(x)$ determines v_x subject to the boundary conditions that $v_x = 0$ for $y = 0$ and $v_x \to U$ for $y \to \infty$. The preceding analysis shows that the solution is generally correct up to terms of order $1/\mathsf{Re}$.

Copyright © 1998–2002, Benny Lautrup

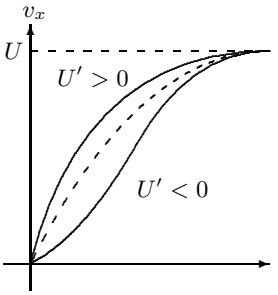

In accelerating flow, $U' > 0$, the wall curvature is negative, whereas in decelerating flow the curvature is positive. The dashed curve sketches the velocity profile for vanishing wall curvature.

The wall curvature

At the wall, $y = 0$, we know that the velocity components must vanish. The first order derivative at the wall $\partial v_x/\partial y|_{y=0}$ determines the wall stress. Putting $y = 0$ in the Prandtl equation (24-26) we get the *wall curvature*

$$\left.\frac{\partial^2 v_x}{\partial y^2}\right|_{y=0} = -\frac{UU'}{\nu} \; . \tag{24-27}$$

If the slip-flow accelerates, $U' > 0$, the wall curvature will be negative and favor the turn-over of the velocity in the boundary layer towards the terminal value, U. Conversely, if the slip-velocity decreases, $U' < 0$, the wall curvature will be positive and adversely affect the turn-over to terminal velocity, leading to an inflection point in the velocity profile. For constant slip-flow, $U' = 0$, the wall curvature vanishes (this is the Blasius case which will be solved exactly in the following section). Higher order derivatives may also be calculated at $y = 0$ by differentiating the Prandtl equation repeatedly after y.

Thickness definitions

In section 24.2 we discussed three precise definitions of thickness for a growing boundary layer based on the wall stress and on the loss in volume and momentum discharge rates caused by the boundary layer. These quantities may also be defined for steady flow but now depend on x rather than t,

$$\sigma_{\mathsf{wall}}(x) = \eta \left.\frac{\partial v_x(x,y)}{\partial y}\right|_{y=0} \; , \tag{24-28a}$$

$$Q(x) = \int_0^\infty (U(x) - v_x(x,y))\, dy \; , \tag{24-28b}$$

$$\dot{\mathcal{P}}_x(x) = \int_0^\infty \rho_0 (U(x) - v_x(x,y)) v_x(x,y)\, dy \; . \tag{24-28c}$$

The wall stress, displacement and momentum thicknesses are defined as before,

$$\frac{1}{\delta_{\,\mathsf{wall}}} = \frac{\sigma_{\mathsf{wall}}}{\eta U} = \frac{1}{U} \left.\frac{\partial v_x}{\partial y}\right|_{y=0} \; , \tag{24-29a}$$

$$\delta_{\mathsf{disp}} = \frac{Q}{U} = \int_0^\infty \left(1 - \frac{v_x}{U}\right) dy \; , \tag{24-29b}$$

$$\delta_{\mathsf{mom}} = \frac{\dot{\mathcal{P}}_x}{\rho_0 U^2} = \int_0^\infty \left(1 - \frac{v_x}{U}\right) \frac{v_x}{U}\, dy \; . \tag{24-29c}$$

Although the thicknesses may be of comparable magnitude, they may vary differently with x, in particular near a separation point.

Copyright © 1998–2002, Benny Lautrup

von Kàrman's integral

It is possible to derive an exact relation between the thicknesses from the Prandtl equation (24-26). Using the continuity equation (24-24), the Prandtl equation may be rewritten in the form,

$$-\nu\frac{\partial^2 v_x}{\partial y^2} = (U-v_x)\frac{dU}{dx} + \frac{\partial[v_x(U-v_x)]}{\partial x} + \frac{\partial[v_y(U-v_x)]}{\partial y} \ ,$$

Integrating this equation over y from 0 to ∞, and using the boundary values $v_y \to 0$ for $y \to 0$ and $U - v_x \to 0$ for $y \to \infty$, we obtain

$$\nu \left.\frac{\partial v_x}{\partial y}\right|_{y=0} = \frac{dU}{dx}\int_0^\infty (U-v_x)\,dy + \frac{d}{dx}\int_0^\infty (U-v_x)v_x\,dy \ . \qquad (24\text{-}30)$$

This is the *von Karman relation* which simply expresses momentum balance in the boundary layer. In terms of the three thicknesses (24-29) it becomes,

$$\boxed{\frac{\nu U}{\delta_{\mathsf{wall}}} = U\frac{dU}{dx}\delta_{\mathsf{disp}} + \frac{d\left(U^2\delta_{\mathsf{mom}}\right)}{dx}} \ . \qquad (24\text{-}31)$$

It plays an important role in approximations to boundary layer flow.

Theodore von Kármán (1881-1963). *Influential Hungarian-American engineer. Lived from 1930 in the US, and became in 1944 cofounder of the Jet Propulsion Laboratory at the California Institute of Technology. Made major contributions to the understanding of fluid mechanics, aircraft structures, rocket propulsion, and soil erosion. A crater on the Moon carries today his name.*

24.4 The Blasius boundary layer

The generic example of a steady laminar boundary layer is furnished by a semi-infinite plate with its edge orthogonal to a uniform flow with constant velocity U, a problem first solved by Blasius in 1908.

Paul Richard Heinrich Blasius (1883–1970). *German physicist, a student of Prandtl. Worked on boundary-layer drag and smooth pipe resistance.*

Self-similarity

As the main variation in v_x happens across the boundary layer, it may be convenient to measure y in units of the thickness of the boundary layer, estimated to be of order $\delta \sim \sqrt{\nu x/U}$ on page 406. Let us for this reason write the velocity in dimensionless form,

$$v_x(x,y) = Uf(s) \ , \qquad s = y\sqrt{\frac{U}{2\nu x}} \ , \qquad (24\text{-}32)$$

where $f(s)$ must satisfy the boundary conditions, $f(0) = 0$ and $f(\infty) = 1$. The factor of 2 in the squareroot is conventional. In principle the function could also depend on the dimensionless variable $\mathsf{Re}_x = Ux/\nu$, but the correctness of the above assumption will be justified by finding a solution satisfying the boundary conditions. Like the growth profile (24-11) this is a self-similar expression. Apart from the overall scale, the velocity field varies in the same way with y for all $x > 0$.

Copyright © 1998–2002, Benny Lautrup

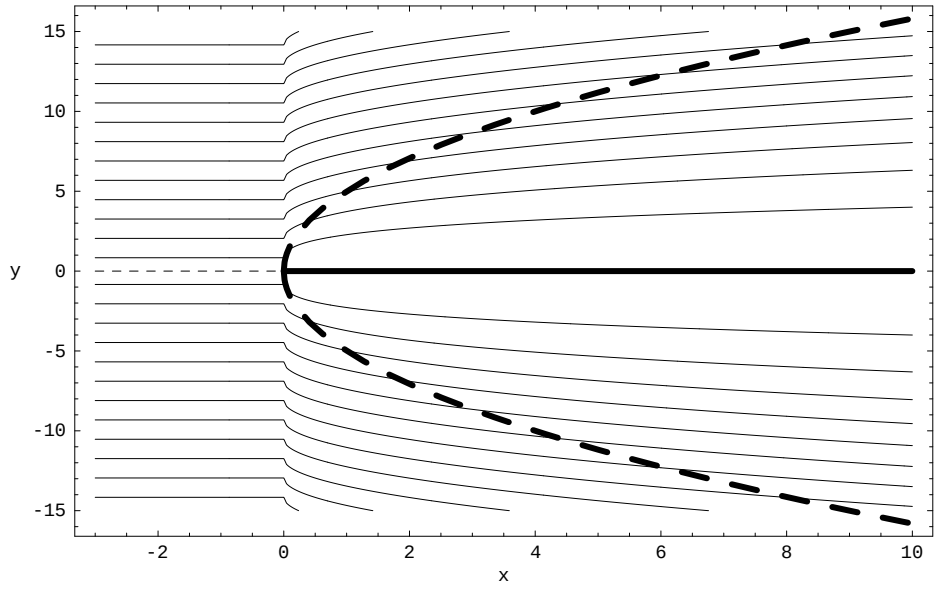

Figure 24.1: *Streamlines around a semi-infinite thin plate with fluid flowing uniformly in from the left (see problem 24.6). Units are chosen so that $U = \nu = 1$. The thin dashed streamline terminates in a stagnation point. The heavy dashed curve indicates the 99% thickness, $y = \delta = 5\sqrt{x}$. The kink in the streamlines at $x = 0$ signals breakdown of the Prandtl approximation in this region.*

Upflow

From the equation of continuity (24-24) we obtain

$$v_y(x,y) = -\frac{\partial}{\partial x}\int_0^y v_x(x,y')\,dy' = -\frac{\partial}{\partial x}\left[\sqrt{2U\nu x}\;g(s)\right] \ .$$

Here we have for convenience defined the integral

$$g(s) = \int_0^s f(s')\,ds' \tag{24-33}$$

so that $f(s) = g'(s)$. Carrying out the differentiation, we obtain the upflow from the layer,

$$v_y(x,y) = h(s)\sqrt{\frac{U\nu}{2x}} \ , \qquad h(s) = sf(s) - g(s) \ . \tag{24-34}$$

The asymptotic value $h(\infty) = \lim_{s\to\infty}(sf(s) - g(s))$ determines the total upflow from the boundary layer into the mainstream.

Copyright © 1998–2002, Benny Lautrup

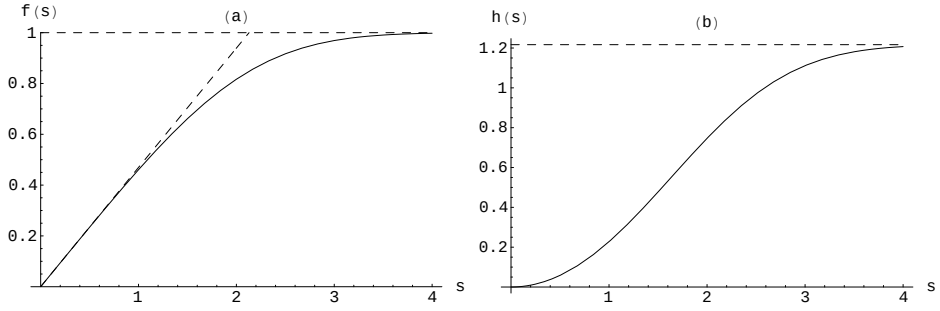

Figure 24.2: *Plot of the self-similar shape functions for (a) $v_x = Uf(s)$, and (b) $v_y = h(s)\sqrt{U\nu/2x}$. The dashed line on pane (a) has slope $f'(0) = 0.469599\ldots$ and is tangent at $s = 0$. The dashed line in pane (b) indicates the asymptotic value $h(\infty) = 1.21678\ldots$ and determines the resulting upwelling of fluid from the boundary layer into the mainstream flow.*

The Blasius equation

Finally, v_y is inserted into the Prandtl equation (24-26) and using that in this case U is constant, we obtain the coupled ordinary differential equations[1]

$$\boxed{f''(s) = -g(s)f'(s)\ , \qquad g'(s) = f(s)\ ,} \tag{24-36}$$

with the boundary conditions $f(0) = 0$, $f(\infty) = 1$ and $g(0) = 0$. If we replace $g(s)$ by s in the first equation, it becomes identical to the Stokes layer equation (24-12).

Numeric integration yields the results shown in fig. 24.1 and 24.2. The condition $f(\infty) = 1$ is a bit troublesome to implement, but one may instead use a "ballistic" approach, where the integration is started with $f(0) = 0$ and $f'(0) = \gamma$, and the correct value of γ is found by searching for the "bulls-eye" $f(\infty) = 1$. The numeric results are $f'(0) = 0.469599\ldots$ and $h(\infty) = 1.21678\ldots$.

Thickness of the Blasius layer

The conventional thickness of the Blasius layer is defined to be the distance $y = \delta$ where the velocity has reached 99% of the slip-flow velocity U, leading to

$$\delta = 3.4719\sqrt{\frac{2\nu x}{U}} = 4.91\sqrt{\frac{\nu x}{U}}\ . \tag{24-37}$$

From (24-29a) we get the wall stress thickness,

$$\delta_{\mathsf{wall}} = \frac{U}{\partial v_x/\partial y|_{y=0}} = \frac{1}{f'(0)}\sqrt{\frac{2\nu x}{U}} \approx 3.012\sqrt{\frac{\nu x}{U}}\ . \tag{24-38}$$

[1]The two differential equations may of course be converted to a single third order differential equation, called the *Blasius equation*

$$g'''(s) = -g(s)g''(s)\ , \tag{24-35}$$

with boundary conditions $g(0) = g'(0) = 0$ and $g'(\infty) = 1$. It is entirely a matter of taste whether to view this equation or (24-36) as being most fundamental.

Copyright © 1998–2002, Benny Lautrup

The velocity at $y = \delta_{\mathsf{wall}}$ is about 85% of its asymptotic value.

The asymptotic upflow $h(\infty) = 0.860394\ldots$ determines the displacement thickness (24-29b) (see problem 24.3)

$$\delta_{\mathsf{disp}} = \sqrt{\frac{2\nu x}{U}} \int_0^\infty (1 - f(s))\, ds = h(\infty)\sqrt{\frac{2\nu x}{U}} \approx 1.7208\sqrt{\frac{\nu x}{U}} \ . \qquad (24\text{-}39)$$

The momentum thickness (24-29c) becomes similarly (see problem 24.4),

$$\delta_{\mathsf{mom}} = \sqrt{\frac{2\nu x}{U}} \int_0^\infty (1 - f(s)) f(s)\, ds = f'(0)\sqrt{\frac{2\nu x}{U}} \approx 0.6641\sqrt{\frac{\nu x}{U}} \ . \qquad (24\text{-}40)$$

The self-similarity guarantees, as for the Stokes layer, that the ratios between the various thicknesses are pure numbers independent of x,

$$\frac{\delta_{\mathsf{wall}}}{\delta_{\mathsf{disp}}} = 1.7503 \ , \qquad \frac{\delta_{\mathsf{wall}}}{\delta_{\mathsf{mom}}} = 4.5355 \ , \qquad \frac{\delta_{\mathsf{disp}}}{\delta_{\mathsf{mom}}} = 2.5912 \ , \qquad (24\text{-}41)$$

That $\delta_{\mathsf{wall}}\delta_{\mathsf{mom}} = 2\nu x/U$ follows in fact from the von Karman relation (24-31).

Friction coefficient

It is customary also to make the wall stress (24-28a) dimensionless by dividing with $\frac{1}{2}\rho_0 U^2$ to get the so-called *local friction coefficient*. For the purely laminar Blasius layer, we have

$$c_f \equiv \frac{\sigma_{\mathsf{wall}}}{\frac{1}{2}\rho_0 U^2} = \frac{2\nu}{U\delta_{\mathsf{wall}}} = \frac{0.664}{\sqrt{\mathsf{Re}_x}} \ , \qquad (24\text{-}42)$$

where as before $\mathsf{Re}_x = Ux/\nu$ is the "downstream" Reynolds number. In turbulent boundary flow, this expression is replaced by a semi-empirical power law (24-44) of the same general form but with a different power and coefficient. Notice the singularity at $x = 0$, which signals breakdown of the boundary layer approximation at the leading edge of the plate.

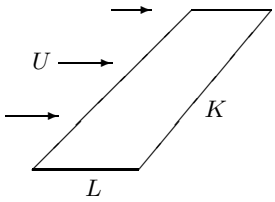

A flat and thin wing aligned with the flow only experiences skin drag.

Laminar skin drag on a flat wing

Consider now an infinitely thin rectangular "wing" with "chord" L in the direction of flow, and a "span" K orthogonal to the flow (in the z-direction). Such an object generates no form drag, when it is aligned with the flow. Disregarding the influence of the rear and side edges of the wing, the total (skin) drag is obtained by integrating $\sigma_{\mathsf{wall}} = \eta U/\delta_{\mathsf{wall}}$ over both sides of the plate,

$$\mathcal{D} = 2\int_0^L \sigma_{\mathsf{wall}}(x)\, K dx = 2\eta U K f'(0) \int_0^L \sqrt{\frac{U}{2\nu x}}\, dx = 4\eta U K f'(0)\sqrt{\frac{UL}{2\nu}} \ .$$

Copyright © 1998–2002, Benny Lautrup

This becomes more transparent when expressed in terms of the dimensionless *drag coefficient* for the wing,

$$C_{\mathcal{D}} = \frac{\mathcal{D}}{\frac{1}{2}\rho_0 U^2 A} = \frac{8f'(0)}{\sqrt{2\mathsf{Re}}} \approx \frac{2.6565}{\sqrt{\mathsf{Re}}}, \tag{24-43}$$

where $A = KL$ is the wing's area and $\mathsf{Re} = UL/\nu$ is its wing's Reynolds number. The skin drag coefficient decreases with the squareroot of the Reynolds number, and is of little importance in most everyday situations with Reynolds number in the millions. The skin drag is mostly dominated by the form drag coefficient which does not decrease but rather stays constant for $\mathsf{Re} \to \infty$.

Example 24.4.1 (Weather vane): A little rectangular metal weather vane with sides $L = 30$ cm and $K = 20$ cm in a 10 m s^{-1} wind has $\mathsf{Re} = UL/\nu \approx 200,000$, well below the onset of turbulence. The drag coefficient becomes $C_{\mathcal{D}} \approx 0.0059$ and the total skin drag $\mathcal{D} \approx 0.018$ N, when the vane aligned with the wind. This drag corresponds to a weight of merely 2 g, whereas the form drag and the other aerodynamic forces that align the vane are much stronger. One should not dimension the support of the vane on the basis of the laminar skin drag!

24.5 Turbulent flat-plate boundary layer

Sufficiently far downstream from the leading edge, the Reynolds number, $\mathsf{Re}_x = Ux/\nu$, will eventually grow so large that the boundary layer becomes turbulent. Empirically, the transition happens for $5 \times 10^5 \lesssim \mathsf{Re}_x \lesssim 3 \times 10^6$, depending on the circumstances, for example the uniformity of the mainstream flow and the roughness of the plate surface. We shall in the following discussion take $\mathcal{R}e_x = 5 \times 10^5$ as the nominal transition point.

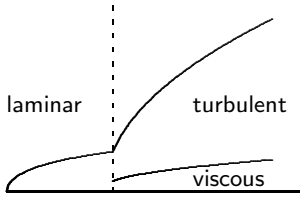

Sketch of the shape of the boundary layer from the leading edge through the transition region. At the transition (dashed line), the turbulent layer grows rapidly whereas the viscous sublayer only grows slowly.

The line of transition across the plate is not a straight line parallel with the z-axis, but rather an irregular, time-dependent, jagged, even fractal interface between the laminar and turbulent regions. This is also the case for the extended interface between the turbulent boundary layer and the fluid at large. Such intermittent and fractal behavior is common to the onset of turbulence in all systems.

Viscous sublayer

In a turbulent boundary layer, the true velocity field $\boldsymbol{v}$ fluctuates in all directions and in time around some mean value. Even very close to the wall, there will be noticeable fluctuations. The no-slip condition nevertheless has to be fulfilled and a thin sublayer dominated by viscous stresses must exist close to the wall. In this viscous sublayer the average velocity $\bar{v}_x$ rises linearly from the surface with a slope, $\partial\bar{v}_x/\partial y|_{y=0} = \bar{\sigma}_{\mathsf{wall}}/\eta$ that can be determined from drag measurements.

A decent semi-empirical expression for the friction coefficient of a turbulent

Copyright © 1998–2002, Benny Lautrup

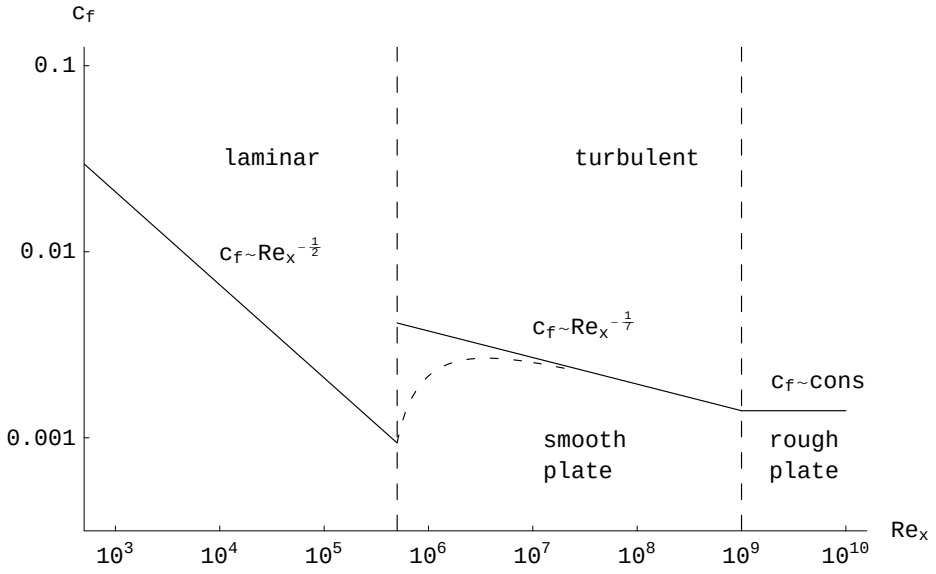

Figure 24.3: *Schematic plot of the local friction coefficient* $c_f = 2\bar{\sigma}_{wall}(x)/\rho_0 U^2$ *across the laminar and turbulent regions as a function of the downstream Reynolds number* $\mathsf{Re}_x = Ux/\nu$. *The transitions at the nominal points* $\mathsf{Re}_x = 5 \times 10^5$ *and* 10^9 *are in reality considerably softer than shown here (with the dashed curve as a possible transition shape). The position of the second transition and the terminal value of* c_f *depend on the roughness of the plate surface (see [36] for details).*

boundary layer is

$$c_f \equiv \frac{\bar{\sigma}_{\mathsf{wall}}}{\frac{1}{2}\rho_0 U^2} \approx \frac{0.027}{\mathsf{Re}_x^{1/7}} \ . \tag{24-44}$$

The turbulent friction coefficient thus decreases much slower than the corresponding laminar friction coefficient (24-42). The two expressions cross each other at $\mathsf{Re}_x \approx 7800$ which is far below the transition to turbulence , implying a jump from $c_f \approx 9.4 \times 10^{-4}$ to $c_f \approx 4.1 \times 10^{-3}$ at $\mathsf{Re}_x \approx 5 \times 10^5$. Turbulent boundary layers thus cause much more skin drag than laminar boundary layers (by a factor of more than 4 at the nominal transition point).

In fig. 24.3 the friction coefficient is schematically plotted across the laminar and turbulent regimes. The transition from laminar to turbulent is in reality not nearly as sharp as shown here, partly because of the average over the jagged transition line. Eventually, for sufficiently large Re_x, the roughness of the plate surface makes the friction coefficient nearly independent of viscosity and thus of Re_x.

The wall stress thickness, $\delta_{\mathsf{wall}} = \eta U/\bar{\sigma}_{\mathsf{wall}}$, which may be taken as a measure of the thickness of the viscous sublayer, becomes in dimensionless form,

$$\frac{U\delta_{\mathsf{wall}}}{\nu} = \frac{2}{c_f} = 74\mathsf{Re}_x^{1/7} \ . \tag{24-45}$$

This "wall Reynolds number" drops from the Blasius value 2000 immediately before the transition to 500 immediately after.

Copyright © 1998–2002, Benny Lautrup

Turbulent drag on a flat wing

Let us again consider a finite "wing" of size $A = L \times K$. For sufficiently large Reynolds number $\mathsf{Re} = UL/\nu$, the boundary layer will always become turbulent some distance downstream from the the leading edge, and the skin drag will in general be dominated by the turbulent boundary layer's larger friction coefficient. Disregarding the drag from the laminar boundary layer near the leading edge, the dimensionless turbulent drag coefficient becomes (including both sides of the plate)

$$C_{\mathcal{D}} = \frac{2}{\frac{1}{2}\rho_0 U^2 A} \int_0^L \bar{\sigma}_{\mathsf{wall}}(x)\, K dx = \frac{0.063}{\mathsf{Re}^{1/7}} \tag{24-46}$$

where $A = KL$ as before is the wing area. If the leading laminar boundary layer cannot be disregarded, this expression is modified (see below).

Example 24.5.1: A 2×2 m^2 flag in a 10 $\mathsf{m\ s}^{-1}$ wind has a Reynolds number of $\mathsf{Re} \approx 1.3 \times 10^6$, well inside the turbulent region. The laminar skin drag coefficient is $C_{\mathcal{D}} \approx 0.0023$ whereas the turbulent skin drag coefficient is $C_{\mathcal{D}} \approx 0.0084$. The turbulent skin drag is only $\mathcal{D} \approx 1.68$ N which seems much too small to keep the flag straight. But flags tend to flap irregularly in the wind, thereby adding a much larger average form drag to the total drag, and giving it even in a moderate wind the nearly straight form that we admire so much. The straight flag in the wind is an image so ingrained in our minds that NASA chose to simulate it when planting an aluminium edition of Stars and Stripes on the airless Moon.

Turbulent momentum thickness

Above the viscous sublayer, there is a much thicker layer of turbulent fluid. The von Karman relation (24-31) expresses momentum balance in the boundary layer, and takes the for constant slip-velocity the form,

$$\frac{d\delta_{\mathsf{mom}}}{dx} = \frac{\nu}{U\delta_{\mathsf{wall}}} = \frac{1}{2} c_f \ , \tag{24-47}$$

independently of whether the boundary layer is laminar or turbulent. Assuming that the turbulent boundary layer covers all the plate, we find by integrating this expression over x from $x = 0$, using (24-44),

$$\frac{U\delta_{\mathsf{mom}}}{\nu} = 0.016 \mathsf{Re}_x^{6/7} \ . \tag{24-48}$$

The shape factor,

$$\frac{\delta_{\mathsf{mom}}}{\delta_{\mathsf{wall}}} = 2.13 \times 10^{-4} \mathsf{Re}_x^{5/7} \ , \tag{24-49}$$

has the value 2.5 at the transition $\mathsf{Re}_x = 5 \times 10^5$ and grows rather fast above. Its dependence on x demonstrates that turbulent boundary layers are not self-similar near the wall.

Copyright © 1998–2002, Benny Lautrup

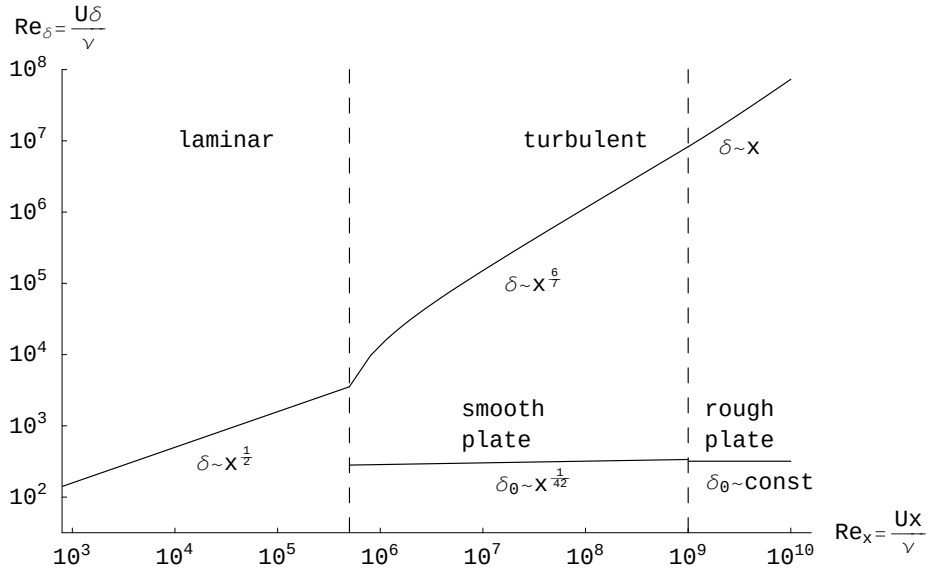

Figure 24.4: *Schematic plot of the dimensionless "true" thickness, represented by* $\mathsf{Re}_\delta = U\delta/\nu$*, as a function of downstream distance* x*, represented by* $\mathsf{Re}_x = Ux/\nu$*. Also shown is the thickness of the viscous sublayer* δ_0*. The momentum thickness* δ_{mom} *is obtained from the refined expression (24-50) and is everywhere roughly a factor 10 smaller than the "true" thickness* δ*. The real transition at the nominal value,* $\mathsf{Re}_x = 5 \times 10^5$*, is even softer than shown here. The transition from smooth to rough plate at* $\mathsf{Re} = 10^9$ *is barely visible.*

Refining the analysis to take into account that the transition from laminarity to turbulence happens at a point x_0 downstream from the leading edge, the momentum thickness becomes after integration of (24-47) from $x = 0$ to x

$$\frac{U\delta_{\mathsf{mom}}}{\nu} = \begin{cases} 0.664\sqrt{\mathsf{Re}_x} & x < x_0 \\ 0.664\sqrt{\mathsf{Re}_{x_0}} + 0.016\left(\mathsf{Re}_x^{6/7} - \mathsf{Re}_{x_0}^{6/7}\right) & x > x_0 \end{cases} \tag{24-50}$$

The momentum thickness thus passes continuously through the transition because it is obtained by integration, in contrast to the wall stress thickness which reflects the (soft) jump in the wall stress. This also provides a more refined expression for the plate drag coefficient, $C_D = 4\ \delta_{\mathsf{mom}}|_{x=L}\,/L$.

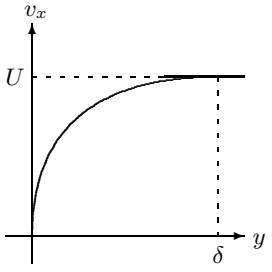

The turbulent velocity profile is approximately a power $\bar{v}_x \sim y^\gamma$ *with* $\gamma \approx 1/7$*. The vertical tangent at* $y = 0$ *is unphysical, because it implies infinite wall stress.*

The "true" thickness of the turbulent boundary layer

The "true" boundary layer thickness δ is, as mentioned before, dependent on convention, even in the laminar (Blasius) case. Empirically, the flat-plate turbulent boundary layer outside the viscous sublayer is decently described by the approximately self-similar model (due to Prandtl),

$$\frac{\bar{v}_x}{U} = \left(\frac{y}{\delta}\right)^{1/7} , \qquad (0 \lesssim y < \delta) \ . \tag{24-51}$$

Copyright © 1998–2002, Benny Lautrup

In calculating the integrated momentum width, we can disregard the thin viscous sublayer, and find by inserting (24-51) into (24-29c) $\delta_{\mathsf{mom}}/\delta = 7/72$, or $\delta = 10.3\delta_{\mathsf{mom}}$. From the turbulent momentum thickness (24-48) we obtain the "true" thickness of the turbulent boundary layer,

$$\boxed{\mathsf{Re}_\delta \equiv \frac{U\delta}{\nu} = 0.16\,\mathsf{Re}_x^{6/7}} \,. \tag{24-52}$$

Since the "true" thickness of the laminar Blasius layer is $\delta = 5\sqrt{\nu x/U} = 7.5\delta_{\mathsf{mom}}$, there is only an insignificant jump in δ at the nominal transition point $\mathsf{Re}_x = 5\times 10^5$. The "true" thickness is displayed schematically in fig. 24.4.

> There is, however, a bit of hidden subtlety in the above argument. By using the average field to calculate δ_{mom} we have ignored the velocity fluctuations in the turbulent layer. From (24-29c), it follows that fluctuations in v_x give a negative contribution to δ_{mom}, so that the correct turbulent momentum thickness is in fact somewhat smaller than what is found in this model.

The "true" thickness of the viscous sublayer

It is also possible to get an estimate of the "true" thickness δ_0 of the viscous sublayer from the intercept between the linearly rising field, $\bar{v}_x/U = y/\delta_{\mathsf{wall}}$, in the sublayer and the power law (24-51). Demanding continuity at $y = \delta_0$, we get

$$\frac{\delta_0}{\delta_{\mathsf{wall}}} = \left(\frac{\delta_0}{\delta}\right)^{1/7} \,.$$

Solving this equation for δ_0 and inserting δ_{wall} from (24-45) and δ from (24-52) we obtain[2]

$$\frac{U\delta_0}{\nu} = 206\mathsf{Re}_x^{1/42} \,. \tag{24-53}$$

At the nominal transition point $\mathsf{Re}_x = 5\times 10^5$, this becomes 282, which grows to 337 at $\mathsf{Re}_x = 10^9$. The sublayer thickness is also plotted in Fig. 24.4 and its variation with Re_x is barely perceptible.

The fraction of the terminal velocity that the fluid has at the "edge" of the sublayer becomes

$$\frac{v_x\big|_{y=\delta_0}}{U} = 2.8\mathsf{Re}_x^{-5/42} \,. \tag{24-54}$$

At the nominal transition point it is 0.59 and falls to 0.24 at $\mathsf{Re}_x = 10^9$.

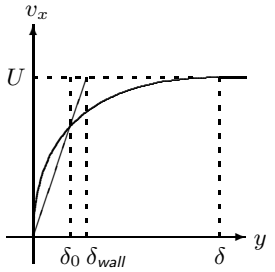

The "true" thickness δ_0 of the viscous sublayer is obtained from the intercept between Prandtl's power profile (24-51) and the linearly rising velocity in the sublayer. The kink at $y = \delta_0$ is unphysical, because it gives rise to a small jump in shear stress that violates Newton's third law (slightly). The real transition from viscous sublayer to turbulent main layer is softer than shown here.

[2] The remarkable 42'nd root may have deeper significance [48].

Copyright © 1998–2002, Benny Lautrup

∗ 24.6 Self-similar boundary layers

In the preceding sections, self-similarity has been an important assumption permitting us to convert the partial differential equations of fluid mechanics into ordinary differential equations. In this section we shall focus on laminar self-similar flows that may be viewed as generalizations of the Blasius solution to non-constant slip-flow, $U(x)$. We shall see that the Prandtl equations only allow certain classes of slip-flows when self-similarity is required.

The Falkner-Skan equation

A self-similar flow is of the form,

$$v_x = U(x)f(s) \ , \qquad s = \frac{y}{\lambda(x)} \ , \tag{24-55}$$

where $f(s)$ is an unknown function, and $\lambda(x)$ sets the scale at the point x. As before, the boundary conditions are $f(0) = 0$ and $f(\infty) = 1$.

It follows immediately from the equation of continuity (24-24) that

$$v_y = -\frac{\partial}{\partial x}\left(U\lambda g\right) \ , \tag{24-56}$$

where as before $g(s) = \int_0^s f(s')ds'$ is the integral of $f(s)$. Substituting v_x and v_y into (24-26) we obtain after a little algebra the coupled ordinary differential equations,

$$f'' = -\alpha g f' - \beta(1 - f^2) \ , \qquad g' = f \ , \tag{24-57}$$

where

$$\alpha = \frac{\lambda\lambda' U + \lambda^2 U'}{\nu} \ , \qquad\qquad \beta = \frac{\lambda^2 U'}{\nu} \ . \tag{24-58}$$

Since f and g by the similarity assumption only depend on s, the coefficients α and β have to be independent of x.

The equations (24-58) may thus be viewed as two coupled ordinary differential equations for λ and U, also parameterized by α and β. To solve them we first notice that they imply $d(\lambda^2 U)/dx = (2\alpha - \beta)\nu$. For $\alpha > 0$ we may without loss of generality rescale λ such that $\alpha = 1$, and with a suitable choice of origin for x we obtain $\lambda^2 U = (2 - \beta)\nu x$ for $\beta \neq 2$. Using this result, we get $\beta = (2 - \beta)xU'/U$, implying that $U \sim x^m$ with $m = \beta/(2 - \beta)$, or conversely $\beta = 2m/(1 + m)$. Putting it all together, the permissible slip-velocity and thickness scale are,

$$U(x) = Ax^m \ , \qquad\qquad \lambda(x) = \sqrt{\frac{(2 - \beta)\nu x}{U(x)}} \ , \tag{24-59}$$

where $A > 0$ and $m = \beta/(2 - \beta)$ are constants.

Copyright © 1998–2002, Benny Lautrup

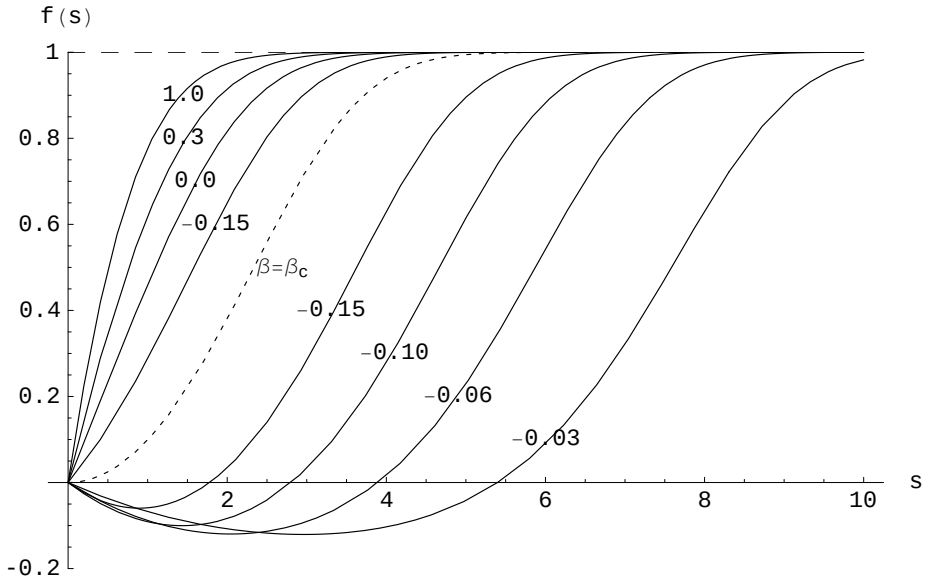

Figure 24.5: *Self-similar Falkner-Skan solutions $f(s)$ for select values of $\beta_c \le \beta \le 1$ where $\beta_c = -0.198838$. The Blasius profile is obtained for $\beta = 0$. Notice that there are two solutions for each value of β in the interval $\beta_c < \beta < 0$, one of which has reversed flow. The critical profile with $\beta = \beta_c$ is shown dashed.*

Again we arrive at two coupled ordinary differential equations[3],

$$\boxed{f'' = -gf' - \beta(1 - f^2) \ , \qquad g' = f \ ,} \tag{24-60}$$

with $\beta = 2m/(1+m)$. Introduced in 1931 by Falkner and Skan[49], these nonlinear equations have since been extensively analyzed [50, 51]. We shall leave as an exercise to discuss the other families of solutions having $\alpha \le 0$ or $\beta = 2$.

Upflow

A non-constant inviscid slip-flow $v_x = U(x)$ generates by itself (and mass conservation) an upflow $v_y = -yU'(x)$. The total upflow, including that of the boundary layer is given by (24-56), from which we get the part due to the boundary layer itself

$$v_y + yU'(x) = h(s)\frac{\nu}{\lambda} \ , \tag{24-61}$$

$$h(s) = sf(s) - g(s) + \beta s(1 - f(s)) \ . \tag{24-62}$$

This reduces to the Blasius result (24-34) for $\beta = 0$. Asymptotically, this function also converges to a finite value, $h(\infty) = \lim_{s\to\infty}(s - g(s))$, depending of course on the value of β.

[3]The two equations may trivially be rewritten as a single third order equation $g''' + gg'' + \beta(1 - g'^2) = 0$. It is purely a matter of taste, which formulation one prefers, but in keeping with the style of this chapter, we shall stick to (24-60).

Copyright © 1998–2002, Benny Lautrup

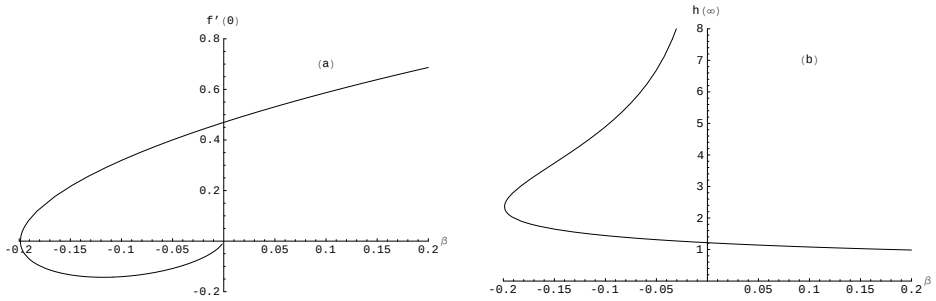

Figure 24.6: **(a)** *The wall slope $f'(0)$ of the Falkner-Skan solutions as a function of m. At the critical point $\beta = \beta_c = -0.198838\ldots$, the slope vanishes with vertical tangent. Notice that the slope has two solution for $\beta_c < \beta < 0$, one with positive and one with negative values. The negative solution joins continuously with the positive at $\beta = \beta_c$ and terminates at $\beta = 0$.* **(b)** *The asymptotic upflow $h(\infty)$ plotted as a function of β.*

Numeric results

Numeric integration of the Falkner-Skan equation is reasonably straightforward using (with some care) the same "ballistic" method of integration as described for the Blasius equation (24-35). The integration process is initiated with $g(0) = f(0) = 0$ and $f'(0) = \gamma$, and a search is made for the value of the slope γ that yields $f(\infty) = 1$. In the same way as there in general are two elevation angles that may be used to hit a target with a cannon, we may expect to find more than one solution to the Falkner-Skan equation for certain values of β.

In fig. 24.5 the velocity profile is shown for a selection of β-values, and in fig. 24.6 the slope $f'(0)$ and the asymptotic upflow $h(\infty)$ are plotted as functions of β in the interval $-0.2 < \beta < 0.2$. The most conspicuous feature of the figures is the existence of two solutions in the interval $\beta_c < \beta < 0$ where $\beta_c = -0.198838\ldots$ (corresponding to $m_c < m < 0$ with $m_c = -0.0904286\ldots$). One solution has positive slope and the other negative. As seen in fig. 24.5, the profiles are markedly different with backflow occurring in the negative solution. The slope vanishes at the critical point $\beta = \beta_c$, where the positive solution joins with the negative.

In the region $0 < \beta < 2$ (*i.e.* $0 < m < \infty$), the slip-velocity increases downstream. The solutions are unique and resemble all the Blasius solution, except that the thickness scale grows slower than $\sqrt{x}$. For $\beta > 1$ (*i.e.* $m > 1$) the layer is suppressed by the accelerating flow and gets thinner with x.

For $-\infty < \beta < 0$ (*i.e.* $-1 < m < 0$), the slip-flow decelerates and the thickness grows faster than $\sqrt{x}$. There are, as mentioned, precisely two solutions in the interval $\beta_c < \beta < 0$. In the interval $-1 < \beta < \beta_c$, there are no solutions at all, but for any β in the interval $-\infty < \beta < -1$ there appears to be from one to three distinct solutions with different values of the slope [51]. All these solutions oscillate and overshoot while converging upon $f(\infty) = 1$. They are of no interest in the context of flat plate boundary layers.

Copyright © 1998–2002, Benny Lautrup

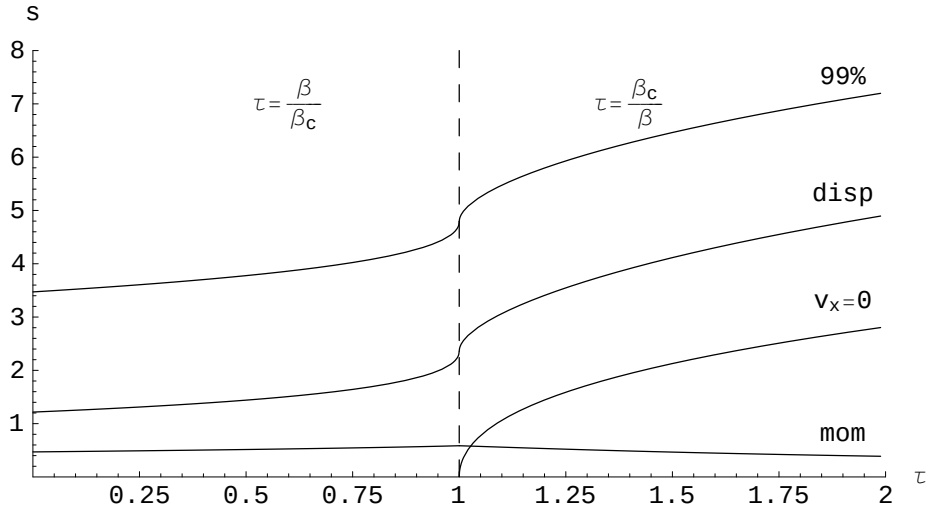

Figure 24.7: *The variation in the thicknesses (in units of λ) across the separation region as a function of the artificial time τ, defined to be $\tau = \beta/\beta_c$ for the branch with positive and $\tau = \beta_c/\beta$ for the branch with negative slope. The Blasius values are obtained for $\tau = 0$ and the transition occurs for $\tau = 1$. There is backflow in the region below the curve marked $v_x = 0$. The curve marked 99% is the conventional thickness.*

Thicknesses

In units of the scale λ, the various thicknesses (24-29) become,

$$\frac{\delta_{\mathsf{wall}}}{\lambda} = \frac{1}{f'(0)} \ , \tag{24-63a}$$

$$\frac{\delta_{\mathsf{disp}}}{\lambda} = \int_0^\infty (1 - f(s))\, ds = h(\infty) \ , \tag{24-63b}$$

$$\frac{\delta_{\mathsf{mom}}}{\lambda} = \int_0^\infty f(s)(1 - f(s))\, ds = \frac{f'(0) - \beta h(\infty)}{1 + \beta} \ . \tag{24-63c}$$

Due to self-similarity their ratios are independent of x. As the rightmost expressions show, it is not necessary to evaluate the integrals as such, because they may be expressed in terms of $f'(0)$ and $h(\infty)$ (see problem 24.7).

Separation?

Self-similar flows can strictly speaking not be used to study separation, because the velocity profile by construction has the same shape everywhere. It nevertheless looks very much as if separation takes place all over the x-axis for $\beta = \beta_c$, where the positive solution without backflow smoothly joins with the negative solution with backflow.

To expose this more clearly we imagine that the exponent $\beta = \beta(\tau)$ is slowly driven towards β_c in an artificial time τ. On the branch with positive slope $f'(0)$ the "time" may conveniently be chosen as $\tau = \beta/\beta_c$, which varies from $\tau = 0$ in the Blasius case, to $\tau = 1$ at the critical point. On the other side of the critical

Copyright © 1998–2002, Benny Lautrup

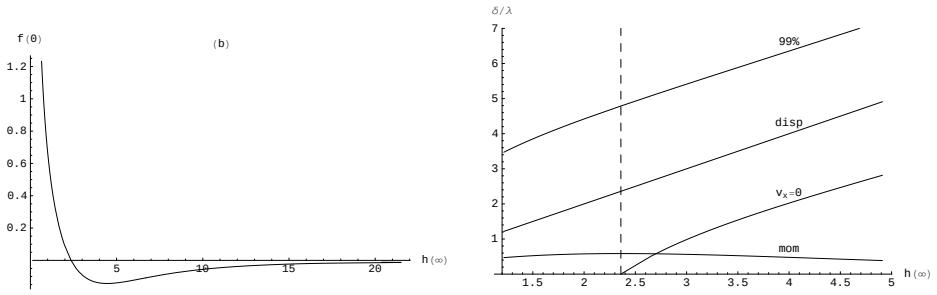

Figure 24.8: **(a)** *The slope $f(0)$ as a function of the asymptotic upflow $h(\infty)$. The slope is smooth across the transition which happens at $h(\infty) = 2.35886\ldots$.* **(b)** *Thicknesses as a function of $h(\infty)$ in the same range of β-values as in fig. 24.7. Notice the absence of a cusp at the transition.*

point, where the slope is negative, we cannot use this definition, because that would drive us back towards $\tau = 0$ along the second branch (see fig. 24.6a). Instead we choose here, quite arbitrarily, $\tau = \beta_c/\beta$, which ranges from $\tau = 1$ at the critical point to $\tau \to \infty$ for $\beta \to 0$.

In fig. 24.7 the thickness variation with τ is shown around the transition at $\tau = 1$. In both branches one may also define the 99% thickness δ_{99}, and in the negative (backflow) branch, one may define the thickness $\delta_{v_x=0}$ from the value of y where $v_x = 0$. The figure gives a believable picture of separation happening at $\tau = 1$, but it is actually a fake. Beyond the transition point we have arbitrarily chosen one definition of "time" which takes the value $\tau = 1$ at the transition and grows monotonously beyond. But we could have chosen otherwise, for example $\tau = (\beta_c/\beta)^2$ or anything else with the right properties. One might even choose $\tau = h(\infty) = \delta_{\mathsf{disp}}/\lambda$ as a "time" that grows smoothly and monotonously as one progresses along both branches (see fig. 24.8).

∗ 24.7 Predicting the separation point

Copyright © 1998–2002, Benny Lautrup

Problems

24.1 a) Show that for constant slip-flow velocity it is possible to obtain a boundary layer of constant thickness on an infinitely extended plate, if fluid is sucked through the plate at a constant rate. b) Discuss what happens if fluid is pushed through instead.

∗ **24.2** Show that for a plate moving with velocity to $U(t)$ for $t > 0$ (and being at rest for $t < 0$) we have the general solution

$$v_x(y,t) = \int_0^t \left(1 - \mathrm{erf}\left(\frac{y}{2\sqrt{2\nu(t-t')}}\right)\right) \frac{dU(t')}{dt'}\, dt' \tag{24-64}$$

24.3 Show that for the Blasius solution

$$\int_0^\infty (1 - f(s))\, ds = h(\infty) \tag{24-65}$$

24.3 Use that $f(s) = g'(s)$ and (24-34) to evaluate the integral

$$\int_0^\infty (1 - f(s))\, ds = \lim_{s\to\infty}(s - g(s)) = \lim_{s\to\infty}(sg'(s) - g(s)) = h(\infty) \tag{24-66}$$

24.4 Show that for the Blasius solution

$$\int_0^\infty f(s)(1 - f(s))\, ds = 2f'(0) \tag{24-67}$$

24.5 Show that well outside the boundary layer but still close to the wall, the continuity equation (24-24) implies that

$$v_y(x,y) = \frac{dQ(x)}{dx} - y\frac{dU(x)}{dx}\ , \qquad \delta \ll y \ll L\ , \tag{24-68}$$

Interpret the two terms.

24.6 The form of the streamlines in Fig. 24.1 may be obtained directly from the Blasius solution. Show that

a) the streamlines are solutions to (with s given by (24-32))

$$\frac{dy}{dx} = \sqrt{\frac{\nu}{Ux}}\left(s - \frac{g(s)}{f(s)}\right) \tag{24-69}$$

b) this may be written

$$\frac{ds}{dx} = -\frac{1}{2x}\frac{g(s)}{f(s)} \tag{24-70}$$

c) a streamline satisfies

$$g(s) = \frac{C}{\sqrt{x}} \tag{24-71}$$

where C is a constant.

Copyright © 1998–2002, Benny Lautrup

d) the explicit solution is

$$y = \sqrt{\frac{\nu x}{U}} g^{-1}\left(y_0 \sqrt{\frac{U}{\nu x}}\right) \tag{24-72}$$

where g^{-1} is the inverse function of g, and y_0 the intercept with the y-axis.

∗ **24.7** Show that for solutions to the Falkner-Skan equation (24-60),

$$I_1 = \int_0^\infty (1 - f(s))\, ds = \lim_{s\to\infty} (s - g(s)) = h(\infty) \tag{24-73}$$

$$I_2 = \int_0^\infty (1 - f(s)) f(s)\, ds = \frac{f'(0) - \beta h(\infty))}{1+\beta} \tag{24-74}$$

Copyright © 1998–2002, Benny Lautrup